Letter

Correlation-enhanced stability of microscopic cyclic heat engines

Guo-Hua Xu [1,*] and Gentaro Watanabe [1,2,†]

[1]Department of Physics and Zhejiang Institute of Modern Physics, Zhejiang University, Hangzhou, Zhejiang 310027, China

[2]Zhejiang Province Key Laboratory of Quantum Technology and Device, Zhejiang University, Hangzhou, Zhejiang 310027, China

(Received 3 December 2021; revised 24 June 2022; accepted 6 July 2022; published 1 August 2022)

For cyclic heat engines operating in a finite cycle period, thermodynamic quantities have intercycle and intracycle correlations. By tuning the driving protocol appropriately, we can get the negative intercycle correlation to reduce the fluctuation of work through multiple cycles, which leads to the enhanced stability compared to the single-cycle operation. Taking the Otto engine with an overdamped Brownian particle as a working substance, we identify a scenario to get such enhanced stability by the intercycle correlation. Furthermore, we demonstrate that the enhancement can be readily realized in the current experiments for a wide range of protocols. By tuning the parameters within the experimentally achievable range, the uncertainty of work can be reduced to below ∼50%.

DOI: 10.1103/PhysRevResearch.4.L032017

Introduction. With advanced technology, various microscopic thermal devices have been fabricated on the submicron scale [1–10]. Among them, an important breakthrough for the exploration beyond conventional macroscopic thermodynamics is the experimental realization of the so-called Brownian heat engine [4–7], which consists of a Brownian particle subject to a time-dependent optical trap. In contrast to conventional macroscopic heat engines, fluctuations of thermodynamic quantities are significant in microscopic heat engines due to the small number of degrees of freedom in their working substance [11,12]. In the past three decades, stochastic thermodynamics has been developed to formulate laws of thermodynamics for the fluctuating thermodynamic quantities of small systems, and has had great success in understanding thermodynamics of small systems [13–16]. Motivated by the experimental realization of microscopic heat engines and the theoretical advances in thermodynamics of small systems, there is a surge of activity on the study of microscopic heat engines [17–32]. Recently, fluctuations of the performance of microscopic heat engines and characterization of their performance beyond the mean values of thermodynamic quantities have become an active research topic [33–49].

Nevertheless, many studies of cyclic heat engines so far consider single-cycle operations and focus on the performance within a single cycle. In these studies, fluctuations of the thermodynamic quantities usually include only the intracycle correlation. In the quasistatic limit, since the thermal noise erases the correlation among thermodynamic quantities in different cycles [13,38], it is sufficient to describe the fluctuations focusing on a single cycle. However, to get the nonzero power output, we need to operate engines in a finite cycle period. In this case, the effect of the intercycle correlation becomes non-negligible. Therefore, for engine operations over multiple cycles, assessing the performance within a single cycle is insufficient. Instead, assessments of the engine performance should address the global process over multiple cycles to include intercycle correlations.

Recently, fluctuations including intercycle correlations also started to be discussed. For example, various properties of the stochastic efficiency have been derived [50–56], and thermodynamic uncertainty relations which give a lower bound of uncertainties of the current [57–64] have been generalized for cyclic heat engines in the long-time limit [62–64].

However, the role of the time correlation in fluctuations of thermodynamic quantities has not been thoroughly explored. Since engines are supposed to operate over multiple cycles consecutively with a finite cycle period in practical situations, there is a great demand for a scheme to prevent the degradation of performance in multiple cycles by the intercycle correlation effect. In this Letter, by clarifying the effect of time correlation of work in microscopic heat engines with a finite cycle period, we identify such a scheme to reduce the fluctuation of work output. Since the fluctuation of work output is comparable to or even bigger than the average of work output in current experiments of small heat engines [4,5], reducing the fluctuation of work output is a crucial issue. Taking an example of the Otto engine using a Brownian particle as a working substance, we demonstrate that the reduction of the fluctuation of work output can be realized in a robust manner in the current experiments, and this reduction can be more than 50%.

Setup. We study a small cyclic heat engine whose working substance is in contact with a heat bath with the controllable temperature $T(t)$ (we set the Boltzmann constant $k_B = 1$

*guohuax@zju.edu.cn
†gentaro@zju.edu.cn

throughout the Letter). The working substance is described by the Hamiltonian $H(\Gamma, t)$ with an external control parameter $\lambda(t)$, where Γ is the microstate of the working substance in the phase space. The engine is driven by time-periodically modulating T and λ with period τ, i.e., $T(t) = T(t+\tau)$ and $\lambda(t) = \lambda(t+\tau)$. Under such a protocol, we assume the engine is already driven into a periodic state with the probability distribution function (PDF) satisfying $p(\Gamma, t) = p(\Gamma, t+\tau)$ after running many cycles [20]. Therefore, we can represent time t by the phase as $\theta = 2\pi t/\tau$, and assign the initial phase θ_0 for the starting point of the cycle.

The work $W_{\theta_0}^{(n)}$ extracted through n cycles with the initial phase θ_0 is a random variable given by

$$W_{\theta_0}^{(n)} = -\int_{\theta_0\tau/2\pi}^{n\tau+\theta_0\tau/2\pi} \frac{\partial H(\Gamma, t)}{\partial \lambda(t)} \dot{\lambda}(t) dt, \tag{1}$$

where the integral follows the Stratonovich rule [13]. The ensemble average $\langle W_{\theta_0}^{(n)} \rangle$ of work is independent of θ_0, and satisfies $\langle W_{\theta_0}^{(n)} \rangle = n \langle W^{(1)} \rangle$, where $\langle \cdots \rangle = \int \mathscr{D}[\Gamma(t)] p[\Gamma(t)] \cdots$ is the path integral over all the possible trajectories $\Gamma(t)$.

The variance of work with initial time $t_0 = \theta_0 \tau/(2\pi)$ is given by

$$\mathrm{Var}\big[W_{\theta_0}^{(n)}\big] = \int_{t_0}^{n\tau+t_0} dt \int_{t_0}^{n\tau+t_0} dt'\, C(t, t'), \tag{2}$$

where the covariance function of power $\dot{W} \equiv -\partial_\lambda H(\Gamma, t)\dot{\lambda}(t)$ is defined as $C(t, t') \equiv \langle \dot{W}(t)\dot{W}(t') \rangle - \langle \dot{W}(t) \rangle \langle \dot{W}(t') \rangle$. The variance $\mathrm{Var}[W_{\theta_0}^{(n)}]$ of work can be given by the sum of the contribution from each cycle, $n\,\mathrm{Var}[W_{\theta_0}^{(1)}]$, and the remaining contribution denoted by $\mathscr{C}_{\theta_0}^{(n)}$:

$$\mathrm{Var}\big[W_{\theta_0}^{(n)}\big] = n\,\mathrm{Var}\big[W_{\theta_0}^{(1)}\big] + \mathscr{C}_{\theta_0}^{(n)}. \tag{3}$$

Here, the first term can be identified as the intracycle correlation within each single cycle and the second term $\mathscr{C}_{\theta_0}^{(n)}$ can be regarded as the intercycle correlation between different cycles. Since the system is not in a steady state, $\mathrm{Var}[W_{\theta_0}^{(n)}]$ changes with θ_0. However, the θ_0 dependence is negligible for $n \to \infty$ because the correlation decays exponentially in time.

In this Letter, we use the single-cycle uncertainty $\Delta_{\theta_0}^{(1)} \equiv \mathrm{Var}[W_{\theta_0}^{(1)}]/\langle W_{\theta_0}^{(1)} \rangle^2$ to describe the fluctuation of work within each single cycle. According to the law of large numbers, the uncertainty of work extracted through a large number n of cycles vanishes as $\sim 1/n$. Therefore, we use the scaled uncertainty Δ^∞ for infinite cycles defined as

$$\Delta^\infty = \lim_{n\to\infty} \Delta_{\theta_0}^{(n)} \equiv \lim_{n\to\infty} n \frac{\mathrm{Var}\big[W_{\theta_0}^{(n)}\big]}{\big\langle W_{\theta_0}^{(n)} \big\rangle^2}. \tag{4}$$

Note that the θ_0 dependence of $\Delta_{\theta_0}^{(n)}$ vanishes in the limit of $n \to \infty$ because $\mathrm{Var}[W_{\theta_0}^{(n)}]$ does so and $\langle W_{\theta_0}^{(n)} \rangle$ is independent of θ_0. The multicycle uncertainty $\Delta_{\theta_0}^{(n)}$ $(n \geqslant 2)$ defined in Eq. (4) is the quantity to be compared with $\Delta_{\theta_0}^{(1)}$. For a large cycle period, where the intercycle correlation is negligible, $\mathscr{C}_{\theta_0}^{(n)} \simeq 0$, $W_{\theta_0}^{(n)}$ is diffusive with $\mathrm{Var}[W_{\theta_0}^{(n)}] = n\,\mathrm{Var}[W_{\theta_0}^{(1)}]$, and we get $\Delta^\infty = \Delta_{\theta_0}^{(1)}$. On the other hand, for a small cycle period comparable to the relaxation time of the working substance, the intercycle correlation is significant. Our goal is to find an appropriate protocol which yields $\Delta^\infty < \Delta_{\theta_0}^{(1)}$ (i.e., $\mathscr{C}_{\theta_0}^{\infty} < 0$) for arbitrary θ_0.

Relation between the single-cycle and multicycle uncertainties. To discuss the relationship between the uncertainties within a single cycle $\Delta_{\theta_0}^{(1)}$ and infinite cycles Δ^∞, we consider an overdamped Brownian particle trapped in a one-dimensional harmonic oscillator potential with the Hamiltonian

$$H(x, t) = \tfrac{1}{2}\lambda(t)\, x(t)^2. \tag{5}$$

Here, $\lambda(t)$ is the stiffness of the potential which serves as a mechanical control parameter and $x(t)$ is the position of the Brownian particle. This system is described by the Ornstein-Uhlenbeck process [65]. The correlation function $\phi(t, t') \equiv \langle x(t)x(t') \rangle$ with $\phi(t, t') = \phi(t', t)$ is derived from the solution of the Itô stochastic differential equation for this process, see Supplemental Material [66]. The resulting correlation function $\phi(t, t')$ for $t < t'$ is given by

$$\phi(t, t') = \phi(t, t) \exp\left[-\mu \int_t^{t'} ds \lambda(s)\right], \tag{6}$$

where μ is the mobility. In addition, since $\phi(t, t)$ is periodic in time, we have

$$\phi(t+\tau, t'+\tau) = \phi(t, t'). \tag{7}$$

The covariance function of power becomes $C(t, t') = \frac{1}{2}\dot{\lambda}(t)\dot{\lambda}(t')\phi(t, t')^2$ [66]. From Eqs. (6) and (7), we get the following properties of the covariance function: $C(t+\tau, t'+\tau) = C(t, t')$ and $C(t, t'+\tau) = aC(t, t')$, where $a \equiv \exp[-2\mu \int_0^\tau dt \lambda(t)] < 1$. Therefore, $C(t, t')$ decays exponentially in time when $|t - t'| \gg \tau$, and the correlation time of work is given by $\tau_{\mathrm{corr}} = 2\mu \int_0^\tau dt \lambda(t)/\tau$.

From the above properties of $C(t, t')$, we can write the intercycle correlation $\mathscr{C}_{\theta_0}^{(2)}$ within the two successive cycles as $\mathscr{C}_{\theta_0}^{(2)} = [a + \gamma(\theta_0)]\mathrm{Var}[W_{\theta_0}^{(1)}]$, where

$$\gamma(\theta_0) \equiv 2 \int_{\tau+t_0}^{2\tau+t_0} dt' \int_{t'-\tau}^{\tau+t_0} dt \frac{C(t, t')}{\mathrm{Var}\big[W_{\theta_0}^{(1)}\big]}. \tag{8}$$

In the same way, we can write $\mathscr{C}_{\theta_0}^{(n)}$ in terms of a, $\gamma(\theta_0)$, and $\mathrm{Var}[W_{\theta_0}^{(1)}]$ [66]. Then, the uncertainty for n cycles reads [66]

$$n\Delta_{\theta_0}^{(n)} = \left[(n - s_n)\frac{1+\gamma(\theta_0)}{1-a} + s_n\right]\Delta_{\theta_0}^{(1)}, \tag{9}$$

where $s_n \equiv (1-a^n)/(1-a) \geqslant 1$. For infinite cycles, we get

$$\frac{\Delta_{\theta_0}^{(1)}}{\Delta^\infty} = \frac{1-a}{1+\gamma(\theta_0)}. \tag{10}$$

For finite n cycles, the uncertainty derived from Eqs. (9) and (10) reads

$$\Delta_{\theta_0}^{(n)} = \left(1 - \frac{s_n}{n}\right)\Delta^\infty + \frac{s_n}{n}\Delta_{\theta_0}^{(1)}. \tag{11}$$

If the intercycle correlation $\mathscr{C}_{\theta_0}^{(2)}$ is negative, i.e., $a + \gamma(\theta_0) < 0$, we get $\Delta_{\theta_0}^{(1)} > \Delta_{\theta_0}^{(n)} > \Delta^\infty$ from Eqs. (10) and (11) [67]. This means that the negative covariance of work between two successive cycles, $\mathscr{C}_{\theta_0}^{(2)} < 0$, indicates the reduction of uncertainty of work in multiple cycles. It is vice versa for

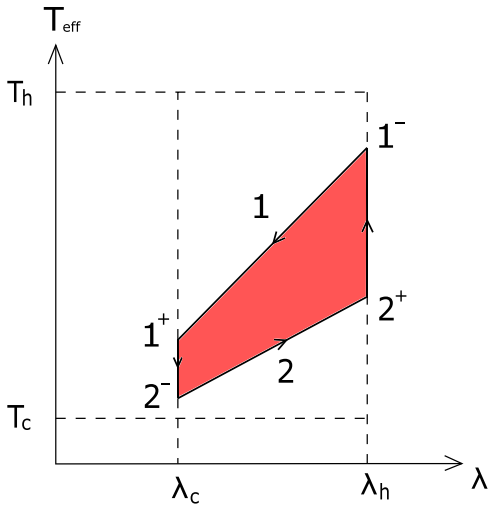

FIG. 1. Brownian Otto cycle with a finite cycle period on the λ-$T_{\rm eff}$ plane. Strokes 1 and 2 are isentropic expansion and compression, respectively. 1^+ (1^-) is the node after (before) the isentropic expansion and 2^+ (2^-) is the node after (before) the isentropic compression. Since the durations of isochoric strokes are finite, the effective temperature at nodes 1^- and 2^- are different from T_h and T_c, respectively.

the positive intercycle correlation. It is noted that the essential point of the above discussion is the exponential decay in time of the correlation functions. Even if the effect of inertia is non-negligible beyond the overdamped limit, the correlation functions can still be exponential in time with a smaller correlation time in the overdamped regime [66]. In addition, in the strongly underdamped regime, the correlation functions can be well approximated by an exponentially decaying function with a large correlation time $\tau_{\rm corr} \simeq \gamma^{-1}$ obtained by averaging over the rapid oscillation [66]. Therefore, for both cases, the above results can still apply, but with a different value of $\tau_{\rm corr}$.

It is possible to observe the enhanced stability due to the negative intercycle correlation when $\tau \lesssim \tau_{\rm corr}$. To show this effect, below we consider a simple Brownian Otto engine, where the analytical result can be obtained. However, a similar result is also obtained for the Carnot cycle [66].

Results for the Brownian Otto cycle. Next, taking the Brownian Otto engine as an example, we demonstrate that the negative intercycle correlation can be realized in a wide range of parameters in the driving protocol. We still consider an overdamped Brownian particle in a harmonic oscillator potential described by the Ornstein-Uhlenbeck process. In this model, since the PDF $p(x,t)$ of any periodic state is Gaussian, we can define the effective temperature $T_{\rm eff}$ of the Brownian particle given by $T_{\rm eff} = \lambda\langle x^2\rangle$ [18]. The Brownian Otto engine consists of two isochoric and two isentropic strokes as shown in Fig. 1 [68]. During the hot (cold) isochoric strokes, the temperature T of the bath and the parameter λ are fixed at T_h and λ_h (T_c and λ_c), respectively, for the duration τ_h (τ_c) with $\lambda_c < \lambda_h$. During the isentropic strokes, T and λ are quenched simultaneously in a way such that the Shannon entropy $S \equiv -\langle \ln p\rangle$ is unchanged [18]. We assume that the isentropic strokes are instantaneous, so that the cycle period is given by $\tau = \tau_h + \tau_c$.

For each mth cycle, we assign an odd integer $i = 2m-1$ for the isentropic expansion stroke and an even integer $i = 2m$ for the isentropic compression stroke (see the strokes labeled "1" and "2" in Fig. 1 for $m = 1$). Since work is done only in the isentropic strokes, the fluctuation of work can take two values depending on whether θ_0 is in the hot or cold isochoric strokes. Therefore, the analysis can be divided into two cases according to the initial phase: The cycle starts before the isentropic expansion or compression. Then, we get the variance of work for the two cases, ${\rm Var}[W^{(1)}_{\rm exp}] = \sum_{i,j=1,2} C_{ij}$ and ${\rm Var}[W^{(1)}_{\rm com}] = \sum_{i,j=2,3} C_{ij}$, respectively. Here, the subscript θ_0 in $W^{(1)}_{\theta_0}$ is replaced by "exp" and "com" for clarity, and $C_{ij} = \frac{1}{2}(\lambda_h - \lambda_c)^2(-1)^{i-j}\phi^2_{ij}$. In this example, the correlation function $\phi_{ij} \equiv \phi(t_i, t_j)$ is analytically solvable [66].

From the analytical solution of ϕ_{ij}, one can find that the uncertainties $\Delta^{(1)}_{\rm exp}$, $\Delta^{(1)}_{\rm com}$, and Δ^{∞} depend on three parameters [66]: $e_h \equiv \exp(-2\mu\lambda_h\tau_h)$, $e_c \equiv \exp(-2\mu\lambda_c\tau_c)$, and $\phi_r \equiv \phi_{11}/\phi_{22}$. Here, e_h and e_c are measures of the incompleteness of the equilibration in the hot and cold isochoric strokes, respectively, and ϕ_r describes the spread of the width of the PDF of the Brownian particle during the hot isochoric strokes. Since we are interested in the heat engine, the mean value of work should be positive, $\langle W^{(1)}\rangle = (\lambda_h - \lambda_c)(\phi_{11} - \phi_{22})/2 > 0$, and thus $\phi_r > 1$. In addition to the condition $\phi_r > 1$, the region of ϕ_r is upper bounded as $\phi_r < 1/e_c$ because the parameters e_h, e_c, and ϕ_r are constrained by [66]

$$\frac{(1-e_h)(1-\phi_r e_c)}{(1-e_c)(\phi_r - e_h)} = R, \tag{12}$$

where $R \equiv T_c\lambda_h/(T_h\lambda_c)$ describes the reversibility with

$$\eta = 1 - \frac{\lambda_c}{\lambda_h} = 1 - \frac{1}{R}\frac{T_c}{T_h} < \eta_C. \tag{13}$$

Since $0 < e_c < 1$, $0 < e_h < 1 < \phi_r$, and $0 < R < 1$, we get $\phi_r < 1/e_c$ from Eq. (12).

Figure 2(a) is a region map showing which of the uncertainties $\Delta^{(1)}_{\rm exp}$, $\Delta^{(1)}_{\rm com}$, and Δ^{∞} is smaller than the others. Regions II and III are of our interest, where the uncertainty Δ^{∞} is smaller than those for a single cycle irrespective of the starting point of the cycle. Figure 2(a) shows that, if the equilibration in the cold isochoric strokes is sufficient with $e_c < 1/\phi_r^2$, we can get the reduction of the uncertainty for multiple cycles. It is noted that, to obtain this reduction, only the degree of equilibration in the cold isochoric strokes matters, but not that in the hot isochoric strokes.

We can provide a physical understanding of Fig. 2(a). An example of the protocol $\lambda(t)$ of the Brownian Otto engine starting before the isentropic expansion (stroke 1) is shown in Fig. 3. The intercycle correlation $\mathscr{C}^{(2)}_{\rm exp} = C_{13} + C_{24} + C_{14} + C_{23}$ is represented by the four lines crossing the boundary between two cycles (vertical dashed line). From Eq. (6), the intercycle correlations in $\mathscr{C}^{(2)}_{\theta_0}$ satisfy $C_{i,i+1} = -e_c C_{ii}$ for odd i and $C_{i,i+1} = -e_h C_{ii}$ for even i. The correlation decays with n as $C_{i,j+2n} = a^n C_{ij}$, where $a = e_c e_h < 1$. Therefore, $\mathscr{C}^{(2)}_{\rm exp}$ is proportional to $C_{11}a - C_{22}e_h \propto \phi_r^2 - 1/e_c$. As we have discussed, the necessary and sufficient condition for the reduction of uncertainty is $\mathscr{C}^{(2)}_{\theta_0} < 0$, which gives $e_c < 1/\phi_r^2$

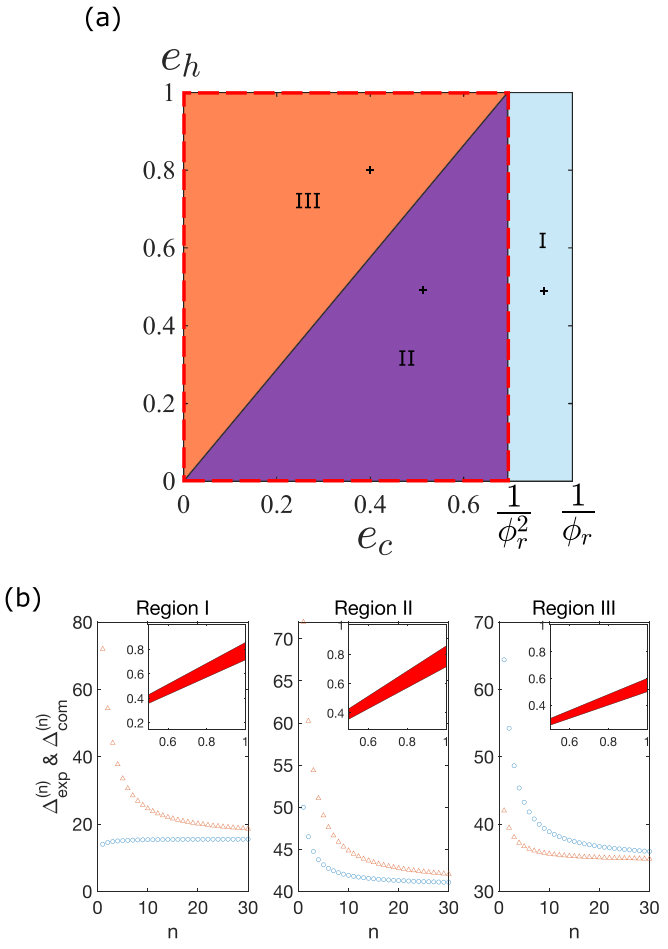

FIG. 2. Mapping out the regions of reduced fluctuation by the intercycle correlation. (a) The three regions with different orders of uncertainties: $\Delta^{(1)}_{com} > \Delta^{\infty} > \Delta^{(1)}_{exp}$ in region I, $\Delta^{(1)}_{com} > \Delta^{(1)}_{exp} > \Delta^{\infty}$ in region II, $\Delta^{(1)}_{exp} > \Delta^{(1)}_{com} > \Delta^{\infty}$ in region III. The uncertainties are reduced by the intercycle correlation in regions II and III, which are enclosed by the red dashed line. Here, we set $\phi_r = 1.2$. (b) $\Delta^{(n)}_{\theta_0}$ as a function of n for a typical point [shown by the cross symbol in (a)] of each region. The blue circles show $\Delta^{(n)}_{exp}$ and the red triangles show $\Delta^{(n)}_{com}$. Insets of (b) show cycle diagrams on the λ-T_{eff} plane for each typical point. Here, we set $T_h = 1$, $\lambda_h = 1$, and $\lambda_c = 0.5$ for all three cycle diagrams.

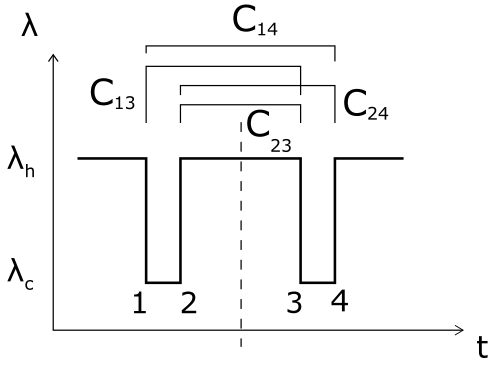

FIG. 3. Schematic diagram showing the contributions from the intercycle correlation for the Brownian Otto cycle starting before the isentropic expansion. Strokes 1 and 3 are isentropic expansion and strokes 2 and 4 are isentropic compression. The vertical dashed line represents the boundary between the cycles.

corresponding to regions II and III. In the same way, for cycles starting before the isentropic compression, the intercycle correlation $\mathscr{C}^{(2)}_{com}$ is given by $\mathscr{C}^{(2)}_{com} \propto 1 - \phi_r^2/e_h$, but it is always smaller than zero. Therefore, we have $\Delta^{\infty} < \Delta^{(1)}_{com}$ for arbitrary e_h. Summarizing the results for the above two cases, we get $\Delta^{\infty} < \Delta^{(1)}_{exp}$ and $\Delta^{(1)}_{com}$ provided $e_c < 1/\phi_r^2$. Namely, the fluctuation of work output is reduced in regions II and III for an arbitrary starting point. The difference between regions II and III is in the ordering of $\Delta^{(1)}_{exp}$ and $\Delta^{(1)}_{com}$ which depends on the intracycle correlation.

Finally, we discuss the role of the temperature of the bath and the experimental feasibility to get the reduction of the fluctuation by the intercycle correlation. First, we consider the mean value of the power P. As obtained in Ref. [71], P depends on six parameters: T_h, T_c, λ_h, λ_c, τ_h, and τ_c [66]. At any point in the region of $0 < e_c < 1$ and $0 < e_h < 1$, the power can be set to any positive value for a given ϕ_r by tuning the remaining free parameters, such as T_h, T_c, and λ_h. Figures 4(b)–4(e) show the power for different values of T_h/T_c. It can be seen that the point in the e_c-e_h plane giving the maximum power can be located in region I or II by tuning T_h/T_c. It is noted that we have $R > T_c/T_h$ for the Otto engine with $P > 0$ ($\eta > 0$) from Eq. (13). Second, we discuss the role of the temperature ratio T_h/T_c in the correlation-enhanced stability. Figure 4(a) shows a contour plot of R as a function of e_c and e_h for a fixed value of ϕ_r. As can be seen from Fig. 4(a), if R is larger than that at $e_c = 1/\phi_r^2$ and $e_h = 0$, it is guaranteed that we are in either region II or III. From Eq. (12), we find that this condition is $R > 1/(\phi_r + 1)$, or

$$\frac{T_c}{T_h} > \frac{\lambda_c/\lambda_h}{\phi_r + 1}. \tag{14}$$

A sufficient condition to satisfy this inequality is $T_h/T_c < 2$, which is easy to realize in experiments. In experiments of microscopic heat engines with Brownian particles [4–6,8,9], one of the heat bath temperatures (commonly T_c) is usually set to be the room temperature: $T_c \sim 300$ K. In such a case, if T_h is 300 K $< T_h <$ 600 K which is indeed the case in typical experiments [4,5], it is guaranteed that the fluctuation of work in the Brownian Otto cycle is always reduced for multiple cycles irrespective of the other parameters. To demonstrate the large reduction of Δ^{∞} by the intercycle correlation, we plot $\Delta^{\infty}/\Delta^{(1)}_{exp}$ and $\Delta^{\infty}/\Delta^{(1)}_{com}$ as functions of T_h/T_c in Fig. 5 for parameter values accessible in current experiments. Since the work output is zero at $T_h/T_c = \lambda_h/\lambda_c$ and increases with T_h/T_c, the region of T_h/T_c shown in Fig. 5 gives positive work output. It is noted that, compared to the above-mentioned sufficient condition, $T_h/T_c < 2$, for $\Delta^{\infty} < \Delta^{(1)}_{exp}$ and $\Delta^{(1)}_{com}$, we can obtain this reduction of Δ^{∞} in a much wider temperature region of $T_h/T_c \lesssim 5.4$. Furthermore, the reduction of Δ^{∞} over the single-cycle uncertainties can be very large by appropriately tuning the parameters and protocol. At $T_h/T_c \simeq 2.3$ where the red and blue lines cross, we have the same reduction rate for an arbitrary starting point. In this case, the uncertainty Δ^{∞} can be reduced to less than 60% of the single-cycle uncertainties. If we set the starting point of the cycle before the isentropic compression stroke (i.e., the case of the red line), Δ^{∞} can be reduced to even below 50% of the single-cycle uncertainty.

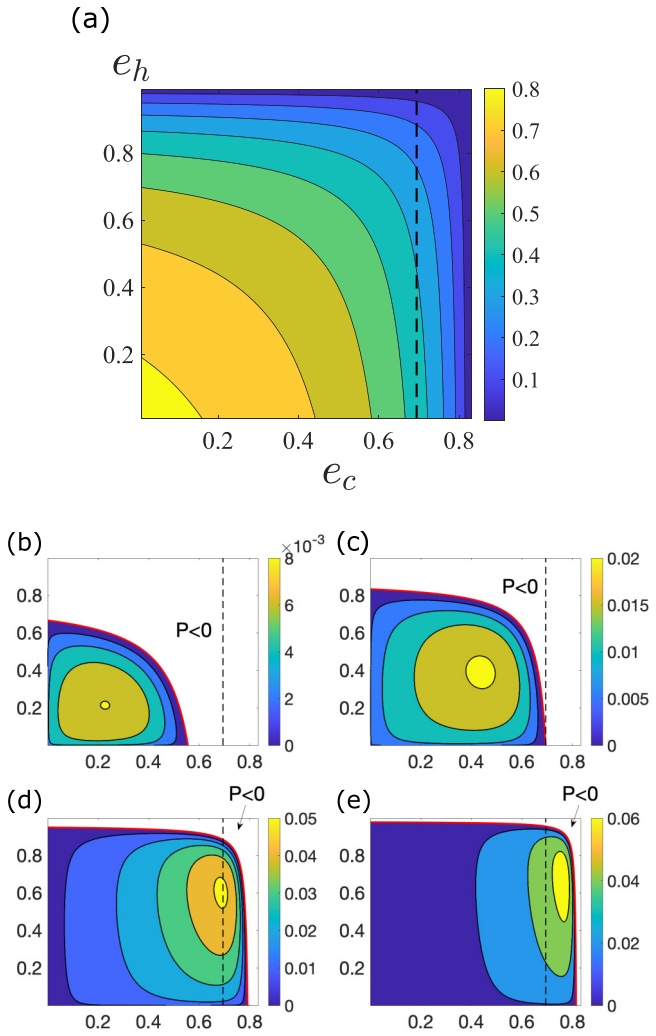

FIG. 4. (a) Product $R \equiv T_c\lambda_h/(T_h\lambda_c)$ of the compression ratio and the temperature ratio as a function of e_c and e_h. (b)–(e) Contour maps of the power as a function of e_c and e_h with given values of T_h/T_c, λ_h, and ϕ_r. Power is in units of $\mu\lambda_h T_h$. We set $T_h/T_c = 1.6$ [for (b)], 2.2 [for (c)], 5 [for (d)], and 10 [for (e)]. The red solid line shows $P = 0$. Since we only focus on the heat engine, values of P for the part with $P < 0$ are not shown here. In each figure, the vertical black dashed line shows $e_c = 1/\phi_r^2$. Here, we set $\phi_r = 1.2$. The contour lines show the values next to the color bar.

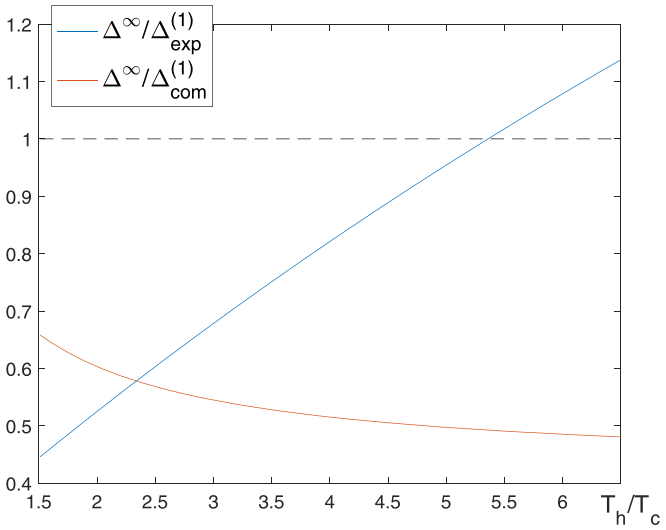

FIG. 5. $\Delta^\infty/\Delta^{(1)}_{\rm exp}$ (blue line) and $\Delta^\infty/\Delta^{(1)}_{\rm com}$ (red line) as functions of T_h/T_c with $T_c = 300$ K. Here, we set $\mu = 0.119\ \mu\text{m pN}^{-1}\,\text{ms}^{-1}$ [69,70], $\lambda_c = 1.6\ \text{pN}\,\mu\text{m}^{-1}$, $\lambda_h = 2.4\ \text{pN}\,\mu\text{m}^{-1}$, $\tau_c = 0.7$ ms, and $\tau_h = 0.3$ ms. These parameters are achievable in the current experiment of Ref. [5]. The ratio $\Delta^\infty/\Delta^{(1)}_{\rm exp}$ is still less than unity even at higher T_h beyond $T_h/T_c = 2$. In addition, the ratios $\Delta^\infty/\Delta^{(1)}_{\rm exp}$ and $\Delta^\infty/\Delta^{(1)}_{\rm com}$ can reach $\lesssim$50%.

Conclusion. Our work has clarified the consequences of time correlation of work over different cycles in cyclic heat engines. If the cycle period is finite, focusing on one cycle is insufficient to discuss fluctuations of the performance of the microscopic heat engines. In particular, taking advantage of the intercycle correlation, the stability of the work output for the multicycle operation can be improved over the single-cycle one. Since such an improvement can be realized in a wide range of protocols, one can further optimize the other performance of the engine (such as efficiency, power, and uncertainty within each cycle). Furthermore, we have demonstrated that our findings can be readily realized in the current experiments. By tuning the parameters within the experimentally achievable range, the uncertainty of work output for infinite cycles can be reduced to less than 50% of the uncertainty for each single cycle. Since the fluctuation of work output can be even larger than the average of the work output in the current experiments [4,5], our result should provide an important step toward the realization of microscopic heat engines for practical use. The effect of time correlation in other kinds of heat engines, such as autonomous heat engines and self-oscillating heat engines [24], is an interesting future problem.

Acknowledgments. G.W. is supported by NSF of China (Grant No. 11975199), by the Zhejiang Provincial Natural Science Foundation Key Project (Grant No. LZ19A050001), and by the Zhejiang University 100 Plan.

[1] T. Hugel, N. B. Holland, A. Cattani, L. Moroder, M. Seitz, and H. E. Gaub, Single-molecule optomechanical cycle, Science **296**, 1103 (2002).

[2] P. G. Steeneken, K. Le Phan, M. J. Goossens, G. E. J. Koops, G. J. A. M. Brom, C. van der Avoort, and J. T. M. van Beek, Piezoresistive heat engine and refrigerator, Nat. Phys. **7**, 354 (2011).

[3] S. Toyabe, T. Sagawa, M. Ueda, E. Muneyuki, and M. Sano, Experimental demonstration of information-to-energy conversion and validation of the generalized Jarzynski equality, Nat. Phys. **6**, 988 (2010).

[4] V. Blickle and C. Bechinger, Realization of a micrometre-sized stochastic heat engine, Nat. Phys. **8**, 143 (2012).

[5] I. A. Martínez, É. Roldán, L. Dinis, D. Petrov, J. M. R. Parrondo, and R. A. Rica, Brownian Carnot engine, Nat. Phys. **12**, 67 (2016).

[6] A. Argun, J. Soni, L. Dabelow, S. Bo, G. Pesce, R. Eichhorn, and G. Volpe, Experimental realization of a minimal microscopic heat engine, Phys. Rev. E **96**, 052106 (2017).

[7] S. Krishnamurthy, S. Ghosh, D. Chatterji, R. Ganapathy, and A. K. Sood, A micrometre-sized heat engine operating between bacterial reservoirs, Nat. Phys. **12**, 1134 (2016).

[8] I. A. Martínez, É. Roldán, L. Dinis, and R. A. Rica, Colloidal heat engines: A review, Soft Matter **13**, 22 (2017).

[9] S. Ciliberto, Experiments in Stochastic Thermodynamics: Short History and Perspectives, Phys. Rev. X **7**, 021051 (2017).

[10] S. Erbas-Cakmak, D. A. Leigh, C. T. McTernan, and A. L. Nussbaumer, Artificial molecular machines, Chem. Rev. **115**, 10081 (2015).

[11] C. Bustamante, J. Liphardt, and F. Ritort, The nonequilibrium thermodynamics of small systems, Phys. Today **58**(7), 43 (2005).

[12] S. Ciliberto, S. Joubaud, and A. Petrosyan, Fluctuations in out-of-equilibrium systems: From theory to experiment, J. Stat. Mech. (2010) P12003.

[13] K. Sekimoto, *Stochastic Energetics* (Springer, Berlin, 2010).

[14] U. Seifert, Stochastic thermodynamics, fluctuation theorems and molecular machines, Rep. Prog. Phys. **75**, 126001 (2012).

[15] U. Seifert, From stochastic thermodynamics to thermodynamic inference, Annu. Rev. Condens. Matter Phys. **10**, 171 (2019).

[16] C. Jarzynski, Equalities and inequalities: Irreversibility and the second law of thermodynamics at the nanoscale, Annu. Rev. Condens. Matter Phys. **2**, 329 (2011).

[17] K. Sekimoto, F. Takagi, and T. Hondou, Carnot's cycle for small systems: Irreversibility and cost of operations, Phys. Rev. E **62**, 7759 (2000).

[18] T. Schmiedl and U. Seifert, Efficiency at maximum power: An analytically solvable model for stochastic heat engines, Europhys. Lett. **81**, 20003 (2008).

[19] V. Holubec, An exactly solvable model of a stochastic heat engine: optimization of power, power fluctuations and efficiency, J. Stat. Mech. (2014) P05022.

[20] K. Brandner, K. Saito, and U. Seifert, Thermodynamics of Micro- and Nano-Systems Driven by Periodic Temperature Variations, Phys. Rev. X **5**, 031019 (2015).

[21] A. Dechant, N. Kiesel, and E. Lutz, All-Optical Nanomechanical Heat Engine, Phys. Rev. Lett. **114**, 183602 (2015).

[22] A. Dechant, N. Kiesel, and E. Lutz, Underdamped stochastic heat engine at maximum efficiency, Europhys. Lett. **119**, 50003 (2017).

[23] C. A. Plata, D. Guéry-Odelin, E. Trizac, and A. Prados, Building an irreversible Carnot-like heat engine with an overdamped harmonic oscillator, J. Stat. Mech. (2020) 093207.

[24] P. Strasberg, C. W. Wächtler, and G. Schaller, Autonomous Implementation of Thermodynamic Cycles at the Nanoscale, Phys. Rev. Lett. **126**, 180605 (2021).

[25] É. Fodor and M. E. Cates, Active engines: Thermodynamics moves forward, Europhys. Lett. **134**, 10003 (2021).

[26] C. Van den Broeck, R. Kawai, and P. Meurs, Microscopic Analysis of a Thermal Brownian Motor, Phys. Rev. Lett. **93**, 090601 (2004).

[27] R. Filliger and P. Reimann, Brownian Gyrator: A Minimal Heat Engine on the Nanoscale, Phys. Rev. Lett. **99**, 230602 (2007).

[28] N. Shiraishi, K. Saito, and H. Tasaki, Universal Trade-Off Relation between Power and Efficiency for Heat Engines, Phys. Rev. Lett. **117**, 190601 (2016).

[29] O. Raz, Y. Subaşı, and R. Pugatch, Geometric Heat Engines Featuring Power that Grows with Efficiency, Phys. Rev. Lett. **116**, 160601 (2016).

[30] M. Esposito, R. Kawai, K. Lindenberg, and C. Van den Broeck, Quantum-dot Carnot engine at maximum power, Phys. Rev. E **81**, 041106 (2010).

[31] O. Abah, J. Roßnagel, G. Jacob, S. Deffner, F. Schmidt-Kaler, K. Singer, and E. Lutz, Single-Ion Heat Engine at Maximum Power, Phys. Rev. Lett. **109**, 203006 (2012).

[32] V. Holubec and R. Marathe, Underdamped active Brownian heat engine, Phys. Rev. E **102**, 060101(R) (2020).

[33] N. A. Sinitsyn, Fluctuation relation for heat engines, J. Phys. A: Math. Theor. **44**, 405001 (2011).

[34] S. Lahiri, S. Rana, and A. M. Jayannavar, Fluctuation relations for heat engines in time-periodic steady states, J. Phys. A: Math. Theor. **45**, 465001 (2012).

[35] M. Campisi, Fluctuation relation for quantum heat engines and refrigerators, J. Phys. A: Math. Theor. **47**, 245001 (2014).

[36] S. Rana, P. S. Pal, A. Saha, and A. M. Jayannavar, Single-particle stochastic heat engine, Phys. Rev. E **90**, 042146 (2014).

[37] Y. Zheng and D. Poletti, Work and efficiency of quantum Otto cycles in power-law trapping potentials, Phys. Rev. E **90**, 012145 (2014).

[38] K. Ito, C. Jiang, and G. Watanabe, Universal bounds for fluctuations in small heat engines, arXiv:1910.08096.

[39] S. Saryal and B. K. Agarwalla, Bounds on fluctuations for finite-time quantum Otto cycle, Phys. Rev. E **103**, L060103 (2021).

[40] S. Saryal, M. Gerry, I. Khait, D. Segal, and B. K. Agarwalla, Universal Bounds on Fluctuations in Continuous Thermal Machines, Phys. Rev. Lett. **127**, 190603 (2021).

[41] K. Brandner and K. Saito, Thermodynamic Geometry of Microscopic Heat Engines, Phys. Rev. Lett. **124**, 040602 (2020).

[42] H. J. D. Miller and M. Mehboudi, Geometry of Work Fluctuations versus Efficiency in Microscopic Thermal Machines, Phys. Rev. Lett. **125**, 260602 (2020).

[43] G. Watanabe and Y. Minami, Finite-time thermodynamics of fluctuations in microscopic heat engines, Phys. Rev. Research **4**, L012008 (2022).

[44] V. Holubec and A. Ryabov, Fluctuations in heat engines, J. Phys. A: Math. Theor. **55**, 013001 (2022).

[45] Y. H. Chen, J.-F. Chen, Z. Fei, and H. T. Quan, A microscopic theory of Curzon-Ahlborn heat engine, arXiv:2108.04128.

[46] A. Dechant and S.-i. Sasa, Current fluctuations and transport efficiency for general Langevin systems, J. Stat. Mech. (2018) 063209.

[47] A. C. Barato and R. Chetrite, Current fluctuations in periodically driven systems, J. Stat. Mech. (2018) 053207.

[48] C. Kwon, J. D. Noh, and H. Park, Work fluctuations in a time-dependent harmonic potential: Rigorous results beyond the overdamped limit, Phys. Rev. E **88**, 062102 (2013).

[49] D. S. P. Salazar, Work distribution in thermal processes, Phys. Rev. E **101**, 030101(R) (2020).
[50] G. Verley, M. Esposito, T. Willaert, and C. Van den Broeck, The unlikely Carnot efficiency, Nat. Commun. **5**, 4721 (2014).
[51] G. Verley, T. Willaert, C. Van den Broeck, and M. Esposito, Universal theory of efficiency fluctuations, Phys. Rev. E **90**, 052145 (2014).
[52] M. Polettini, G. Verley, and M. Esposito, Efficiency Statistics at All Times: Carnot Limit at Finite Power, Phys. Rev. Lett. **114**, 050601 (2015).
[53] J.-H. Jiang, B. K. Agarwalla, and D. Segal, Efficiency Statistics and Bounds for Systems with Broken Time-Reversal Symmetry, Phys. Rev. Lett. **115**, 040601 (2015).
[54] K. Proesmans, B. Cleuren, and C. Van den Broeck, Stochastic efficiency for effusion as a thermal engine, Europhys. Lett. **109**, 20004 (2015).
[55] L. P. Fischer, P. Pietzonka, and U. Seifert, Large deviation function for a driven underdamped particle in a periodic potential, Phys. Rev. E **97**, 022143 (2018).
[56] S. K. Manikandan, L. Dabelow, R. Eichhorn, and S. Krishnamurthy, Efficiency Fluctuations in Microscopic Machines, Phys. Rev. Lett. **122**, 140601 (2019).
[57] A. C. Barato and U. Seifert, Thermodynamic Uncertainty Relation for Biomolecular Processes, Phys. Rev. Lett. **114**, 158101 (2015).
[58] T. R. Gingrich, J. M. Horowitz, N. Perunov, and J. L. England, Dissipation Bounds All Steady-State Current Fluctuations, Phys. Rev. Lett. **116**, 120601 (2016).
[59] J. Horowitz and T. Gingrich, Thermodynamic uncertainty relations constrain non-equilibrium fluctuations, Nat. Phys. **16**, 15 (2020).
[60] P. Pietzonka and U. Seifert, Universal Trade-Off between Power, Efficiency, and Constancy in Steady-State Heat Engines, Phys. Rev. Lett. **120**, 190602 (2018).
[61] V. Holubec and A. Ryabov, Cycling Tames Power Fluctuations near Optimum Efficiency, Phys. Rev. Lett. **121**, 120601 (2018).
[62] A. C. Barato, R. Chetrite, A. Faggionato, and D. Gabrielli, Bounds on current fluctuations in periodically driven systems, New J. Phys. **20**, 103023 (2018).
[63] T. Koyuk, U. Seifert, and P. Pietzonka, A generalization of the thermodynamic uncertainty relation to periodically driven systems, J. Phys. A: Math. Theor. **52**, 02LT02 (2019).
[64] T. Koyuk and U. Seifert, Operationally Accessible Bounds on Fluctuations and Entropy Production in Periodically Driven Systems, Phys. Rev. Lett. **122**, 230601 (2019).
[65] C. W. Gardiner, *Handbook of Stochastic Methods*, 3rd ed. (Springer, Berlin, 2004).
[66] See Supplemental Material at http://link.aps.org/supplemental/10.1103/PhysRevResearch.4.L032017 for details of the derivation or discussion.
[67] In this particular model, the signs of $\mathscr{C}^{(2)}_{\theta_0}$ and $\mathscr{C}^{\infty}_{\theta_0}$ are the same, so that the conditions $\mathscr{C}^{(2)}_{\theta_0} < 0$ and $\mathscr{C}^{\infty}_{\theta_0} < 0$ for $\Delta^{\infty} < \Delta^{(1)}_{\theta_0}$ are equivalent.
[68] In experiments of the Brownian heat engines, adiabatic strokes are often replaced by isentropic strokes [5,8,72] since the working substance is always in contact with the environment (water), so that it is impossible to thermally isolate from the environment. In these isentropic strokes, the parameter λ and the temperature are controlled to keep the mean value of the entropy of the working substance constant.
[69] P. Mestres, I. A. Martínez, A. Ortiz-Ambriz, R. A. Rica, and É. Roldán, Realization of nonequilibrium thermodynamic processes using external colored noise, Phys. Rev. E **90**, 032116 (2014).
[70] From the viscosity η at room temperature $\eta = 0.89\,\mathrm{pN}\mu\mathrm{m}^{-2}$ and the radius of the Brownian particle $r = 0.5\,\mu$m given by Ref. [69], the mobility μ is obtained by $\mu = 1/(6\pi\eta r)$.
[71] G.-H. Xu, C. Jiang, Y. Minami, and G. Watanabe, Relation between fluctuations and efficiency at maximum power for small heat engines, arXiv:2204.09939.
[72] I. A. Martínez, É. Roldán, L. Dinis, D. Petrov, and R. A. Rica, Adiabatic Processes Realized with a Trapped Brownian Particle, Phys. Rev. Lett. **114**, 120601 (2015).